Single Remote Sensing Image Dehazing

Jiao Long, Zhenwei Shi, Wei Tang and Changshui Zhang

Abstract

Remote sensing images are widely used in various fields. However, they usually suffer from the poor contrast caused by haze. In this letter, we propose a simple but effective way to eliminate the haze effect on remote sensing images. Our work is based on the dark channel prior and a common haze imaging model. In order to eliminate halo artifacts, we use a low-pass Gaussian filter to refine the coarse estimated atmospheric veil. We then redefine the transmission, with the aim at preventing the color distortion of the recovered images. The main advantage of the proposed algorithm is its fast speed while it can also achieve good results. The experimental results demonstrate that our algorithm produces visually appealing dehazing images and retains the very fine details. Moreover, for images containing partly clear and partly hazy areas, our algorithm can also achieve good results.

Index Terms

Remote Sensing, Image Dehazing, Dark Channel, Gaussian Filter

I. Introduction

With the advantages of rich information, high spatial resolution and stable geometric location, remote sensing images have been widely used in various fields including agriculture, forestry, hydrology and military. Widespread use of remote sensing images is predicated on high quality images. However, remote sensing is usually vulnerable to weather effects [1], [2]. In general, remote sensing images are taken at a considerable distance from the earth's surface. Consequently, electromagnetic energy cannot reach the sensor before it passes through a substantial atmospheric path. During propagation, the incoming energy interacts with the atmosphere. Some atmospheric effects, such as haze, fog, smoke and cloud, degrade the quality of the received images [3]. In this letter, we address remote sensing images degraded by haze. Images taken under haze conditions often lack visual vividness and appeal, and moreover, they are characterized by a poor visibility of the scene.

The work was supported by the National Natural Science Foundation of China under the Grants 61273245 and 91120301, the 973 Program under the Grant 2010CB327904, the open funding project of State Key Laboratory of Virtual Reality Technology and Systems, Beihang University (Grant No. BUAA-VR-12KF-07), and Program for New Century Excellent Talents in University of Ministry of Education of China under the Grant NCET-11-0775. The work was also supported by Beijing Key Laboratory of Digital Media, Beihang University, Beijing 100191, P.R. China.

Jiao Long, Zhenwei Shi and Wei Tang are with Image Processing Center, School of Astronautics, Beihang University, Beijing 100191, P.R. China (E-mail: shizhenwei@buaa.edu.cn).

Changshui Zhang is with State Key Laboratory on Intelligent Technology and Systems, Tsinghua National Laboratory for Information Science and Technology (TNList), Department of Automation, Tsinghua University, Beijing 100084, P.R. China. E-mail: zcs@mail.tsinghua.edu.cn.

Persistent haze seriously affects the interpretation and the use of remote sensing images. It not only reduces the effectiveness and availability of the remote sensing data, but also puts an obstacle to aerial photography. Therefore, it is imperative to include a mechanism that removes the haze in order to make remote sensing images more reliable. However, haze removal (or dehazing) is not a trivial task because it is an under-constrained problem if the input is only a single hazy image [4], [5].

In recent years, an increasing attention has been paid to develop methods that remove haze from remote sensing images. As a result, a number of scene based algorithms are available to remove haze from the visible bands. Richter proposed a haze removal algorithm using a haze/clear transition region [6]. Du et al. removed the haze using wavelet transform analysis techniques[3]. Zhang et al. developed a haze optimized transformation (HOT) to detect and remove the haze region from Landsat TM/ETM+ archives [7]. Moro and Halounova removed haze region successfully from IKNOS imageries based on an improved haze removal algorithm [8].

In the present work, haze removal is performed on the basis of the method, which is dark channel prior, originally proposed by He et al. [4]. On the basis of the dark channel prior, we propose a simple but effective method for haze removal. Unlike He et al.'s work which uses soft matting method to refine the transmission, we refine the atmospheric veil with a low-pass Gaussian filter. In order to eliminate the color distortion and oversaturated areas in the restored images, we recompute the transmission, which can achieve good results and sufficient speed.

In this letter, we present a fast and physical-based method for single remote sensing image dehazing. It will be shown that restored images are consistent with the original images and visually appealing. The remaining letter is organized as follows. In section II, a brief analysis of haze imaging model is introduced. In section III, a detailed description of our algorithm is given. In section IV, experimental results and a comparison with He et al. [4] are shown. Finally, conclusions are drawn in Section V.

II. Background

When observing scenes captured from an elevated position, features appear to become brighter as they shift toward the horizon. This phenomenon is called airlight [9], which is caused by the scattering of environmental light toward the observer. The radiance of airlight increases with the sensor-to-earth distance d from the object:

$$\mathbf{A}(\mathbf{x}) = \mathbf{A}_{\infty}(1 - e^{-\beta(\mathbf{x})d}), \tag{1}$$

where $\mathbf{x}$ represents the location of a pixel $\mathbf{x} = (x, y)$, β is the attenuation coefficient [10] due to scattering and absorption, and $\mathbf{A}_{\infty}$ is a constant airlight color vector. In satellite remote sensing, the airlight is usually termed path radiance. The attenuation coefficient β [11] describes the incoming energy's attenuation by aerosols. As the attenuation coefficient has the unit (1/km), it has to be multiplied with the constant distance d (km) to yield a pure number in the exponential function. But since the sensor-to-earth distance d is nearly constant, d really is not an additional processing parameter, and the only relevant quantity is the product $\gamma(\mathbf{x}) = \beta(\mathbf{x})d$, which is the optical thickness due to attenuation. So the exponential function in (1) can be written as $e^{-\gamma(\mathbf{x})}$.

Alternatively, introducing $\gamma(\mathbf{x})$ as the attenuation coefficient, and $\beta(\mathbf{x}) = \gamma(\mathbf{x})d$, we will have the exponential function

$$e^{-\beta(\mathbf{x})} \tag{2}$$

and the symbol β can be used as before in the existing equations.

In addition to the presence of airlight, the observed intensity is also influenced by the direct transmission $\mathbf{D}(\mathbf{x})$ [9]:

$$\mathbf{D}(\mathbf{x}) = \mathbf{J}(\mathbf{x})e^{-\beta(\mathbf{x})}, \tag{3}$$

where $\mathbf{J}(\mathbf{x})$ represents the scene radiance.

Therefore, the overall intensity at the sensor is the sum of the airlight and the direct transmission:

$$\mathbf{I}(\mathbf{x}) = \mathbf{D}(\mathbf{x}) + \mathbf{A}(\mathbf{x}). \tag{4}$$

Let $\mathbf{t}(\mathbf{x})$ denote the medium transmission

$$\mathbf{t}(\mathbf{x}) = e^{-\beta(\mathbf{x})}, \tag{5}$$

which describes the portion of the light that is not scattered and not absorbed and reaches the camera. In fact, $\mathbf{t}(\mathbf{x})$ is the direct transmittance, and the diffuse transmittance is neglected. Since the medium transmission $\mathbf{t}(\mathbf{x})$ just depends on pixel position but not on the channel, it does not correspond to the wavelength-depending physical atmospheric transmission. Therefore, we rename it into adjusted image-derive transmission (hereafter, referred to as simply transmission). Moreover, for all RGB channels, their transmissions are the same.

Then haze imaging model [12] can be expressed as:

$$\mathbf{I}(\mathbf{x}) = \mathbf{J}(\mathbf{x})\mathbf{t}(\mathbf{x}) + \mathbf{A}_\infty(1 - \mathbf{t}(\mathbf{x})), \tag{6}$$

where $\mathbf{I}(\mathbf{x})$ represents the observed intensity, $\mathbf{J}(\mathbf{x})$ is the scene radiance. In (6), only the input image $\mathbf{I}$ is known, and we need to recover $\mathbf{J}$, $\mathbf{t}$ and $\mathbf{A}_\infty$. With one equation and three unknowns in (6), dehazing is an ill-posed problem.

Theoretically, the scene radiance can be easily calculated when the transmission and the global atmospheric light are known, which can be written as

$$\mathbf{J}(\mathbf{x}) = \mathbf{A}_\infty - \frac{\mathbf{A}_\infty - \mathbf{I}(\mathbf{x})}{\mathbf{t}(\mathbf{x})}. \tag{7}$$

III. Single Image Dehazing

In this section, we describe our method in detail. First we present a detailed description of dark channel prior of the haze-free outdoor images.

A. Dark Channel Prior

The dark channel prior, which was discovered by He et al. [4], is based on the following observation of outdoor haze-free images: In most of the nonsky patches, pixels in at least one color channel (r, g or b) have a low intensity value and are even close to zero. For an image $\mathbf{J}$, we define its dark channel $\mathbf{J}^{dark}$ as

$$\mathbf{J}^{dark}(\mathbf{x}) = \min_{\mathbf{y}\in\Omega(\mathbf{x})} (\min_{c\in\{r,g,b\}} \mathbf{J}^c(\mathbf{y})), \tag{8}$$

where $\mathbf{J}^c$ is a color channel of $\mathbf{J}$ and $\Omega(\mathbf{x})$ is a local patch centered at $\mathbf{x}$. According to dark channel prior [4], for an outdoor haze-free image $\mathbf{J}$, the intensity of its dark channel image $\mathbf{J}^{dark}$ is very low and close to zero except for the sky region. To verify how good the dark channel prior is on remote sensing images, we manually pick out 1,000 haze-free remote sensing images from the Google Earth. Then we resize these images to 500×600 pixels and calculate their dark channel images with a patch size of 15×15 pixels. Fig. 1 shows several remote sensing images and the corresponding dark channels.

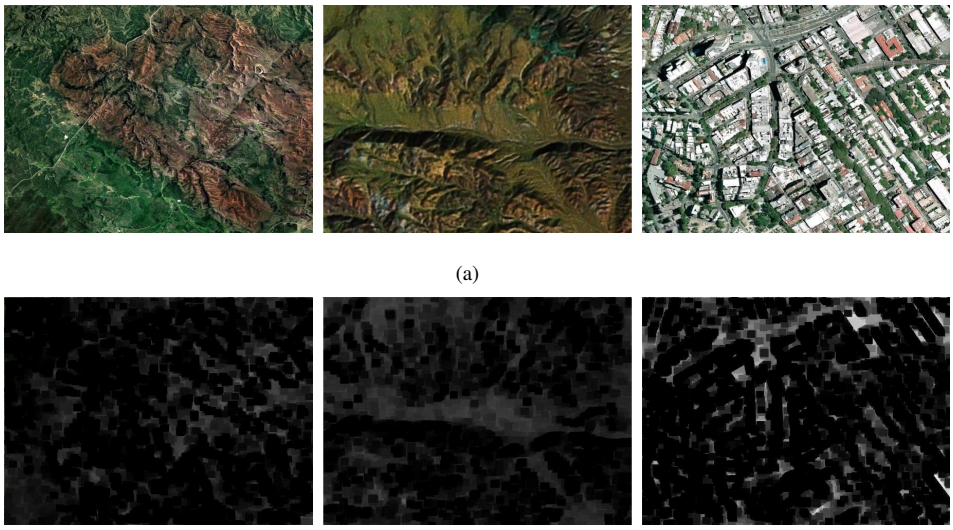

(a)

(b)

Fig. 1. (a) Remote sensing images. (b) The corresponding dark channels.

Fig. 2 is the intensity histogram over all 1,000 dark channels, from which we can see that the intensity of about 74 percent of the pixels in the dark channels is below 25, and the intensity of more than 90 percent of the pixels is below 50. The results indicate that the dark channel prior is valid on remote sensing images.

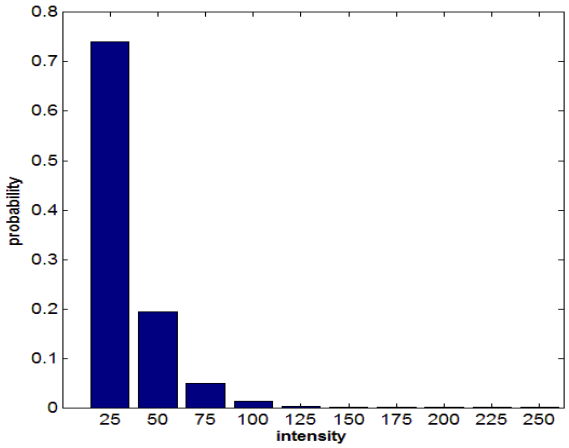

Fig. 2. Histogram of the intensity of the pixels in all of the 1,000 dark channels (each bin stands for 25 intensity levels).

However, as for the images taken under haze condition, the dark channel prior becomes invalid. Affected by the additive airlight, pixels in haze regions have high values in all color channels and the minimal intensity of local patches is high. Therefore, the dark channel of a hazy image will have higher intensity in regions with denser haze. Visually, the intensity of the dark channel is a rough approximation of the thickness of the haze [5].

B. Estimate the Atmospheric Light

According to (4), the airlight becomes more dominant as the distance from the object to the observer increases. The haze imaging model indicates that for two objects with different radiant energy, located at the same distance from the observer, have the same airlight. As observed by Narasimhan and Nayar [13], the atmospheric light $\mathbf{A}_\infty$ is best estimated in the most haze-opaque region. In this letter, we first choose the top 0.1 percent brightest pixels in the dark channel as the most haze-opaque region. Then the value of $\mathbf{A}_\infty$ is extracted from the original hazy image from the same location as its dark channel image, the brightest pixel in the original image $\mathbf{I}$ is considered as the global atmospheric light. This approach is more reliable than only searching for the single brightest pixel in the entire image.

C. Estimate the Coarse Atmospheric Veil

We first define the atmospheric veil $\mathbf{V}(\mathbf{x})$ [14], [15] as follows

$$\mathbf{V}(\mathbf{x}) = 1 - \mathbf{t}(\mathbf{x}). \tag{9}$$

Obviously, the transmission $\mathbf{t}(\mathbf{x}) = e^{-\beta d(\mathbf{x})}$ is within (0,1). Therefore, the atmospheric veil $\mathbf{V}(\mathbf{x})$ is also within the (0,1) interval. The atmospheric veil presents the additive airlight to the scene imaging, and moreover, it is an increasing function with the distance $d(\mathbf{x})$ from the object to the observer. Putting (9) into (6), the haze imaging model (6) can be rewritten as

$$\mathbf{I}(\mathbf{x}) = \mathbf{J}(\mathbf{x})\mathbf{t}(\mathbf{x}) + \mathbf{A}_\infty \mathbf{V}(\mathbf{x}). \tag{10}$$

According to Subsection B, the global atmospheric light $\mathbf{A}_\infty$ can be automatically estimated. In (10), we normalize the haze imaging model by dividing the global atmospheric light $\mathbf{A}_\infty^c$ in each color channel separately,

$$\frac{\mathbf{I}^c(\mathbf{x})}{\mathbf{A}_\infty^c} = \frac{\mathbf{J}^c(\mathbf{x})}{\mathbf{A}_\infty^c}\mathbf{t}(\mathbf{x}) + \mathbf{V}(\mathbf{x}). \tag{11}$$

The value of $\mathbf{A}_\infty$ is not the maximum in the original hazy image, which will cause the fraction $\frac{\mathbf{I}^c(\mathbf{x})}{\mathbf{A}_\infty^c}$ to be greater than 1 for pixels whose intensities are higher than the atmospheric light $\mathbf{A}_\infty$. So we further restrict the normalized image $\frac{\mathbf{I}^c(\mathbf{x})}{\mathbf{A}_\infty^c}$ into [0,1] with linear stretch method.

Therefore, the haze imaging model can be rewritten as

$$\frac{\mathbf{I}(\mathbf{x})}{\mathbf{A}_\infty} = \frac{\mathbf{J}(\mathbf{x})}{\mathbf{A}_\infty}\mathbf{t}(\mathbf{x}) + \mathbf{V}(\mathbf{x}). \tag{12}$$

According to (11), the atmospheric veil $\mathbf{V}(\mathbf{x})$ is subject to two constraints [14]:

1) $\mathbf{V}(\mathbf{x})$ is positive;

2) $\mathbf{V}(\mathbf{x})$ could not be higher than the min color component of $\frac{\mathbf{I}(\mathbf{x})}{\mathbf{A}_\infty}$, which is $\mathbf{V}(\mathbf{x}) \leq \frac{\mathbf{I}(\mathbf{x})}{\mathbf{A}_\infty}$.

First we assume that the atmospheric veil and transmission in a local patch $\Omega(\mathbf{x})$ are constant. Denote the atmospheric veil and transmission as $\tilde{\mathbf{V}}(\mathbf{x})$ and $\tilde{\mathbf{t}}(\mathbf{x})$ respectively, then we take the minimum operation to both three color channels and the local patch on the haze imaging model (12):

$$\min_{\mathbf{y}\in\Omega(\mathbf{x})}(\min_{c\in\{r,g,b\}}\frac{\mathbf{I}^c(\mathbf{y})}{\mathbf{A}_\infty^c}) = \tilde{\mathbf{t}}(\mathbf{x})\min_{\mathbf{y}\in\Omega(\mathbf{x})}(\min_{c\in\{r,g,b\}}\frac{\mathbf{J}^c(\mathbf{y})}{\mathbf{A}_\infty^c}) + \tilde{\mathbf{V}}(\mathbf{x}). \tag{13}$$

According to the dark channel prior, the dark channel of $\mathbf{J}(\mathbf{x})$ is close to zero:

$$\mathbf{J}^{dark}(\mathbf{x}) = \min_{\mathbf{y}\in\Omega(\mathbf{x})}(\min_{c\in\{r,g,b\}}\mathbf{J}^c(\mathbf{y})) = 0. \tag{14}$$

As $\mathbf{A}_\infty^c$ is always positive, this leads to:

$$\min_{\mathbf{y}\in\Omega(\mathbf{x})}(\min_{c\in\{r,g,b\}}\frac{\mathbf{J}^c(\mathbf{y})}{\mathbf{A}_\infty^c}) = 0. \tag{15}$$

Putting (15) into (13), we can extract the atmospheric veil simply by:

$$\tilde{\mathbf{V}}(\mathbf{x}) = \min_{\mathbf{y}\in\Omega(\mathbf{x})}(\min_{c\in\{r,g,b\}}\frac{\mathbf{I}^c(\mathbf{y})}{\mathbf{A}_\infty^c}). \tag{16}$$

In this letter, we only compute the minimum color channel, which aims at preserving a maximum amount of detail, to get the coarse atmospheric veil, which is

$$\tilde{\mathbf{V}}(\mathbf{x}) = \min_{c\in\{r,g,b\}}\frac{\mathbf{I}^c(\mathbf{x})}{\mathbf{A}_\infty^c}. \tag{17}$$

D. Refine the Atmospheric Veil using Gaussian Filter

In Subsection C, we roughly estimated the atmospheric veil $\mathbf{V}(\mathbf{x})$ by taking the minimum operation of the image $\frac{\mathbf{I}(\mathbf{x})}{\mathbf{A}_\infty}$, which could result in $\mathbf{V}(\mathbf{x})$'s discontinuity even if no abrupt depth discontinuities occur. Therefore, to avoid halo artifacts in the restored image, a smooth operation needs to be taken on the coarse atmospheric veil.

In this work, we use a low-pass Gaussian filter to refine the atmospheric veil. Gaussian filter is a nonlinear filter which can smooth images. We smooth the atmospheric veil using a low-pass Gaussian filter, and the refined atmospheric veil $\mathbf{V}(\mathbf{x})$ can be expressed as

$$\mathbf{V}(\mathbf{x}) = \frac{1}{W^g} \sum_{\mathbf{y} \in S} \mathbf{G}_\sigma(\|\mathbf{x} - \mathbf{y}\|) \tilde{\mathbf{V}}(\mathbf{y}), \tag{18}$$

where W^g is the sum weight of the local patch centered at pixel $\mathbf{x}$

$$W^g = \sum_{\mathbf{y} \in S} \mathbf{G}_\sigma(\|\mathbf{x} - \mathbf{y}\|). \tag{19}$$

Here G is a Gaussian function,

$$G_\sigma(x) = e^{-x^2/2\sigma^2}, \tag{20}$$

and the parameter σ represents the size of the neighborhood used to smooth a pixel. A large σ will smooth more, that is, it combines values from more distant image locations [16]. We fix it to 2 for all results in this letter. According to the low-pass Gaussian filter, those pixels closer to the centered pixel $\mathbf{x}$ will get larger weights.

With the refined atmospheric veil, the transmission can be easily calculated according to (9),

$$\mathbf{t}(\mathbf{x}) = 1 - \mathbf{V}(\mathbf{x}). \tag{21}$$

E. Recover the Haze-free Image

With the obtained global atmospheric light and transmission, the scene radiance can be recovered. However, since the coarse atmospheric veil $V(\mathbf{x})$ is estimated using the minimum component on the image $\frac{\mathbf{I}(\mathbf{x})}{\mathbf{A}_\infty}$, the difference between the image $\frac{\mathbf{I}(\mathbf{x})}{\mathbf{A}_\infty}$ and the coarse atmospheric veil $V(\mathbf{x})$ is close to zero with great probability. Therefore, we introduce a constant parameter k to limit the difference. On the other hand, the minimum value of our original transmission calculated by (21) could be very small and even close to zero, which can be seen from the middle-left image of Fig. 3. Thus, the recovered scene radiance is prone to noise. Therefore, it is necessary to restrict the transmission by a lower bound t_0. Actually, t_0 and k are fixed to 0.1 and 0.9 respectively for all results in this letter. The scene radiance $\mathbf{J}(\mathbf{x})$ can be restored by

$$\mathbf{J}(\mathbf{x}) = \mathbf{A}_\infty \times \frac{\mathbf{I}(\mathbf{x})/\mathbf{A}_\infty - k\mathbf{V}(\mathbf{x})}{max(\mathbf{t}(\mathbf{x}), t_0)}. \tag{22}$$

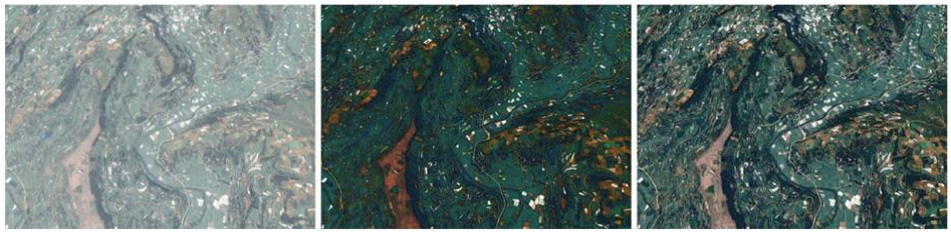

(a)

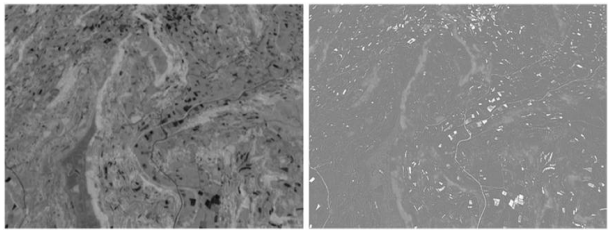

(b)

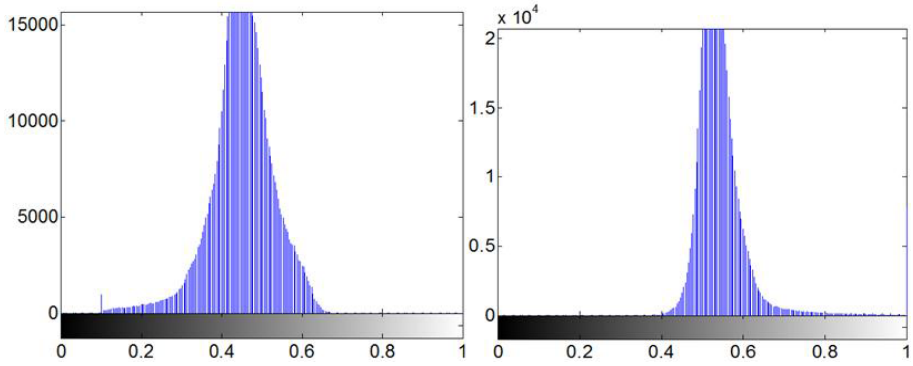

(c)

Fig. 3. From left to right: (a) Initial hazy image, original result and our restored result. (b) Original transmission and refined transmission. (c) Histogram of original transmission and histogram of refined transmission.

The top-middle image of Fig. 3 shows the recovered haze-free image from an input haze remote sensing image in top-left image of Fig. 3. The result reveals that the recovered image is oversaturated and a portion of the detail of the scene is lost. Moreover, the recovered color deviates from the color of the original scene. Actually, the inconsistency results from our estimated atmospheric veil obtained by (17) before using the Gaussian filter.

Regardless of the dark channel prior, the accurate atmospheric veil is

$$\tilde{\mathbf{V}}(\mathbf{x}) = 1 - \frac{1 - \min\limits_{\mathbf{y}\in\Omega(\mathbf{x})} (\min\limits_{c\in\{r,g,b\}} \frac{\mathbf{I}^c(\mathbf{y})}{\mathbf{A}^c_\infty})}{1 - \min\limits_{\mathbf{y}\in\Omega(\mathbf{x})} (\min\limits_{c\in\{r,g,b\}} \frac{\mathbf{J}^c(\mathbf{y})}{\mathbf{A}^c_\infty})}. \tag{23}$$

According to (17), we use a patch size of 1×1 pixel to estimate the atmospheric veil. In fact, the minimum component of the r, g, b channel of the haze-free image cannot be zero. In other word, $\min\limits_{\mathbf{y}\in\Omega(\mathbf{x})} (\min\limits_{c\in\{r,g,b\}} \frac{\mathbf{J}^c(\mathbf{y})}{\mathbf{A}^c_\infty})$ will not be close to zero when the patch size is 1×1 pixel. Therefore, the actual atmospheric veil $\mathbf{V}_{actual}(\mathbf{x})$ is smaller than $\tilde{\mathbf{V}}(\mathbf{x})$ which is estimated using the dark channel prior. Furthermore, in bright regions such as white objects

and water surface, the dark channel prior is invalid because their intensities are large even on clear days. The possibility that $\min_{\mathbf{y}\in\Omega(\mathbf{x})}(\min_{c\in\{r,g,b\}}\frac{\mathbf{J}^c(\mathbf{y})}{\mathbf{A}^c_\infty})$ be close to zero is very low. Thus, the estimated atmospheric veil is larger than the accurate one, i.e., the transmission estimated using the dark channel prior is smaller than the actual one. According to (22), the difference between the color channels will be magnified several times after dividing the small transmission $\mathbf{t}$ even if $\mathbf{I}^r$, $\mathbf{I}^g$, $\mathbf{I}^b$ are very close to each other [17]. As a result, the recovered color could deviate from the original scene and the recovered haze-free image could look unnatural.

In order to eliminate the color distortion, we redefine the transmission $\mathbf{t}(\mathbf{x})$. First, we compute the difference between the color channel of the image $\frac{\mathbf{I}(\mathbf{x})}{\mathbf{A}_\infty}$ and the global atmospheric light $\mathbf{A}_\infty$, and threshold it using a predefined value M. If the difference is smaller than M, we recompute the transmission,

$$\mathbf{t}'(\mathbf{x}) = min(max(M/|\mathbf{I}(\mathbf{x})/\mathbf{A}_\infty - \mathbf{A}_\infty|, 1)\cdot\mathbf{t}(\mathbf{x}), 1), \tag{24}$$

where $\mathbf{t}(\mathbf{x})$ is the refined transmission as (21) and the threshold M is obtained experimentally. According to (24), a brighter pixel will get higher transmission. For remote sensing images in our paper, we have tested the threshold M from 0 to 200 with the step size of 5. It turns out that 125 is good enough for images plagued by constant haze level in our paper. However, for different remote sensing images with varying degrees of haze effect, the threshold may be different.

Then the atmospheric veil is

$$\mathbf{V}'(x) = 1 - \mathbf{t}'(x). \tag{25}$$

For bright regions the intensity of the pixels of which is larger than that of the global atmospheric light, their corresponding transmission is high. Actually, this phenomenon is caused by our recomputed transmission by (24). According to (24), the transmission of the bright regions whose intensity is close to the global atmospheric light will get large value. The bottom-right image of Fig. 3 shows the histogram of our refined transmission, from which we can see that the value of the refined transmission mostly ranges from 0.4 to 0.8. Moreover, the intensity of more than 98 percent of the pixels in the transmission is between 0.4 and 0.9, which is consistent with the physical atmospheric transmittance.

Then the final scene radiance $\mathbf{J}(\mathbf{x})$ can be easily restored by

$$\mathbf{J}(\mathbf{x}) = \mathbf{A}_\infty \times \frac{\mathbf{I}(\mathbf{x})/\mathbf{A}_\infty - k\mathbf{V}'(\mathbf{x})}{\mathbf{t}'(\mathbf{x})}. \tag{26}$$

By deducing (26), the recovered scene radiance also can be written as

$$\mathbf{J}(\mathbf{x}) = \frac{\mathbf{I}(\mathbf{x}) - k\mathbf{A}_\infty}{\mathbf{t}'(\mathbf{x})} + k\mathbf{A}_\infty. \tag{27}$$

Equation (27) indicates that low transmission in bright regions, the intensity of whose pixels is larger than the global atmospheric light, will result in the overflow of the recovered scene radiance in the corresponding areas. And this will also cause loss of details and color distortion. On the other hand, a much better result can be obtained with our refined transmission. The top-right image of Fig. 3 shows the improved recovered haze-free image. As

can be observed, we are able to enhance the contrast of the image while retaining very fine details. Furthermore, our method accurately preserves the color of the objects in the scene.

Fig. 4. Comparison with He's work [4]. (a) Input hazy image. (b) He's result. (c) Our result.

Fig. 5. (a) Input hazy image. (b) Our result.

IV. Experiments Results

To demonstrate the effectiveness of our algorithm, we manually pick out several remote sensing images from the Google Earth and do experiments on these hazy images. For an image of size 600×400 pixels, it takes 0.736s to process on a PC with a 3.2GHz Intel Core i5 Processor using Matlab 2010a. And the recovered image is visually appealing.

Fig. 4 shows a comparison between results obtained by He et al. [4] and our algorithm. Fig. 4 (b) shows the result obtained by He et al. [4], which can retain most of the details while its color is not consistent with the original one. Fig. 4 (c) displays the recovered image obtained by our algorithm, which preserves the color of the objects in the scene. Fig. 5(a) shows a remote sensing image containing partly clear and partly hazy areas. Fig. 5 (b) shows the recovered image obtained by our approach. It can be seen that our results retain very fine details and preserve the color of the original scene.

V. Conclusion

In this work, we present a simple but effective method for single remote sensing image haze removal. Our dehazing technique works well without producing halo artifacts and is very fast. Based on the dark channel prior, we can automatically extract the global atmospheric light and roughly estimate the atmospheric veil. We then refine the atmospheric veil using a low-pass Gaussian filter. In order to eliminate the color distortion of the recovered image,

we recompute the transmission. With the global atmospheric light and the transmission, we are able to produce a haze-free image. We then simulate experiments to validate our algorithm. Remote sensing images recovered are visually appealing, which retain the very fine details and preserve the color of the original scene with low processing time. Moreover, for images containing partly clear and partly hazy areas, our algorithm can achieve good results. However, the primary drawback of our method is that it may lose effectiveness for images with large haze gradients. Therefore, our further research aims at removing remote sensing images with strong haze gradients.

VI. Acknowledgement

The authors would like to thank the anonymous reviewers for their insightful comments and valuable suggestions.

References

[1] X. Wen, X. Yang, "Haze removal from the visible bands of CBERS remote sensing data," 2009 International Conference on Industrial and Information Systems, pp. 118-121, 2009.

[2] Y. Zheng, H. Li, H. Gu, H. Feng, "Research on the haze removal method and parallel implementation for HJ-1 satellite data," International Conference on Multimedia Technology, pp. 1-4, 2010.

[3] Y. Du, B. Guindon, and J. Cihlar. "Haze detection and removal in high resolution satellite image with wavelet analysis," IEEE Transactions on geoscience and remote sensing, vol. 40, no. 1, pp. 210-217, 2002.

[4] K. He, J. Sun, and X. Tang, "Single image haze removal using dark channel prior," IEEE Conference on Computer Vision and Pattern Recognition, pp. 1956-1963, 2009.

[5] K. He, J. Sun, and X. Tang, "Single image haze removal using dark channel prior," IEEE Transactions on Pattern Analysis and Machine Intelligence, vol. 33, no. 12, pp. 2341-2353, Dec. 2011.

[6] R. Richter, "Atmospheric correction of satellite data with haze removal including a haze/clear transition region," Computers Geosciences, vol. 22, pp. 675-681, 1996.

[7] Y. Zhang, B. Guindon, J.Cihlar. "An image transform to characterize and compensate for spatial variations in thin cloud contamination of Landsat images," Remote Sensing of Environment, 82, pp.173-187, 2002.

[8] G. D. Moro and L. Halounova, "Haze removal for high-resolution satellite data: a case study," International Journal of Remote Sensing, vol. 28, pp. 2187-2205, 2007.

[9] H. Koschmieder, "Theorie der horizontalen sichtweite," Beitr. Phys. Freien Atm., vol. 12, pp. 171-181, 1924.

[10] S.G. Narasimhan and S.K. Nayar, "Chromatic framework for vision in bad weather," Proc. CVPR, pp. 598-605, 2000.

[11] A. J. Preetham, P. Shirley, B. Smits, "A practical analytic model for daylight," In ACM SIGGRAPH, pp. 91-100, 1999.

[12] S.G. Narasimhan and S.K. Nayar, "Vision and the atmosphere," Int'l J.Computer Vision, vol. 48, pp. 233-254, 2002.

[13] S.G. Narasimhan and S.K. Nayar, "Contrast restoration of weather degraded images," IEEE Trans. Pattern Analysis and Machine Intelligence, vol. 25, no. 6, pp. 713-724, June 2003.

[14] Tarel J.P., Hautiere N. "Fast visibility restoration from a single color or gray level image," IEEE International Conference on Computer Vision Kyoto, pp. 2201-2208, 2009.

[15] J. Yu, D. Li, Q. Liao, "Physics-based fast single image fog removal," Acta Automatica Sinica, vol. 37, no. 2, pp. 143-149, Feb. 2011(in Chinese).

[16] C. Tomasi, R. Manduchi,"Bilateral filtering for gray and color images," IEEE International Conference on Computer Vision, pp. 839-846, 1998.

[17] J. Jiang, T. Hou, M. Qi, "Improved algorithm on image haze removal using dark channel prior," Journal of circuits and systems, vol. 16, no. 2, pp. 7-12, 2011(in Chinese).